Chapter 4

Unimodal head-width distribution of the European eel (*Anguilla anguilla* L.) from the Zeeschelde does not support disruptive selection

4.1   Abstract

Since the early 20th century, European eels have been dichotomously classified into 'narrow' and 'broad' heads. These morphs are mainly considered the result of a differential food choice, with narrow heads feeding primarily on small/soft prey and broad heads on large/hard prey. Yet, such a classification implies that head-width variation follows a bimodal distribution, leading to the assumption of disruptive selection. We investigated the head morphology of 272 eels, caught over three consecutive years (2015 – 2017) at a single location in the Zeeschelde (Belgium). Based on our results, BIC favoured a unimodal distribution, while AIC provided equal support for a unimodal and a bimodal distribution. Notably, visualization of the distributions revealed a strong overlap between the two normal distributions under the bimodal model, likely explaining the ambiguity under AIC. Consequently, it is more likely that head-width variation followed a unimodal distribution, indicating there are no disruptive selection pressures for bimodality in the Zeeschelde. As such, eels could not be divided in two distinct head-width groups. Instead, their head widths showed a continuum of narrow to broad with a normal distribution. This pattern was consistent across all maturation stages studied here.

4.2   Introduction

Törlitz' (1922) introduction of the terms 'narrow' and 'broad' headed eels (genus *Anguilla*) led to numerous studies trying to explain these two distinct morphs (Fig. 4.1). It was even hypothesised that both morphs had different

life strategies, such as the hypothesis that broad head eels would not migrate to the sea for spawning or even be sterile (Ehrenbaum, 1930; Feddersen) or belonged to different species (Yarrell, 1831). Eels are highly flexible species with a complex life cycle. They develop as leptocephalus larvae into glass eels in the oceans, and settle as elvers in coastal and/or freshwater habitats where they grow during what is commonly known as the yellow eel stage. When eels have reached a threshold size and physiological condition, including sufficient fat reserves, they migrate back to their spawning site as silver eels (Tesch 2003).
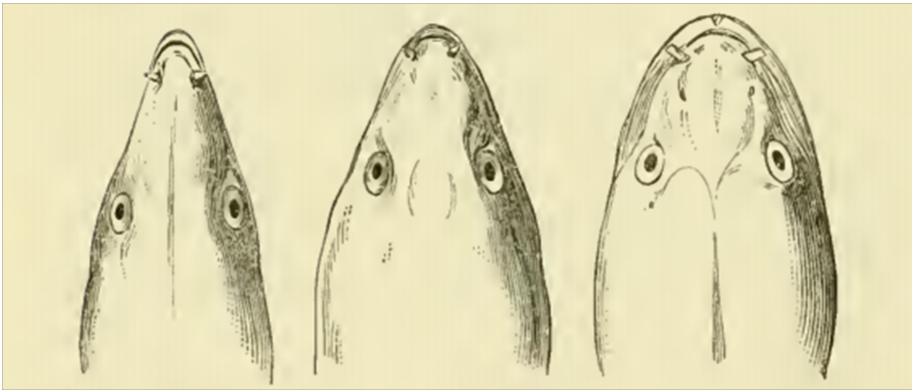

Figure 4.1: Illustration of different head width morphs with, from left to right, a narrow-headed eel, an intermediate-headed eel and a broad-headed eel (figure adopted from Benecke (1880)).

A plausible explanation for the head dimorphism is disruptive selection via resource polymorphism resulting in phenotypic plasticity, a phenomenon that occurs in many vertebrates, especially fish (Skulason and Smith, 1995), and that essentially enables individuals of the same species to reduce intraspecific competition through resource selectivity (Schoener, 1974; Svanbäck et al.,

2008). Differences in consumed prey, for example, can lead to morphological variation in the feeding apparatus. Such a relation between feeding ecology and morphology of the feeding apparatus has been well established in animals (Iijima, 2017; Muschick et al., 2011; Saunders and Barclay, 1992). A similar relation between feeding ecology and morphology has been observed in both the European and Japanese eel. Several studies have illustrated a link between feeding strategy and head width, with narrow-headed eels feeding on small and/or soft prey (e.g. amphipods and chironomids) and broad-headed eels on large and/or hard prey (e.g. molluscs and fish) (Cucherousset et al., 2011; De Meyer et al., 2016; Ehrenbaum, 1930; Kaifu et al., 2013; Lammens and Visser, 1989; Proman and Reynolds, 2000). The broader heads thus reflect better developed jaw closing muscles and a relatively broader skull, features which facilitate the consumption of hard and/or large prey items (De Meyer et al., 2016).

Yet, the European eel is an opportunistic animal (Lammens et al., 1985; Schulze et al., 2004; Van Liefferinge et al., 2012), though specialization on specific prey items has been observed (Barak and Mason, 1992), challenging the dichotomous and strongly deterministic characterization into 'broad' and 'narrow' heads based on feeding behaviour. Indeed, head dimorphism may not be entirely attributed to differences in foraging. For instance, narrow headed Japanese eels grow faster than broad heads (Kaifu et al., 2013) and genetic support for this hypothesis has recently been found in European eel (De Meyer et al., 2017b). Moreover, certain genes involved in growth speed, such as *growth hormone-1*, are also involved in salinity preference (Iwata et al., 1990); thus, eels preferring freshwater grow more slowly than eels favouring marine waters (Edeline et al., 2005). Hence, the basis for head dimorphism in eels may

be much more complex than originally thought. Despite substantial research related to eel head widths, many knowledge gaps remain. For instance, head width of glass eels follows a unimodal distribution (De Meyer et al., 2015). Consequently, a strict dichotomous division of such glass eels into a narrow and a broad headed morph is impossible, as a gradual transition exists from narrower to broader headed eels with many intermediate forms. Still, many studies have dichotomously classified narrow and broad headed eels using a ratio-based threshold: eels with a head width over total body length ratio smaller than 0.033 are considered narrow heads, while eels with larger ratios are broad heads (Barry et al., 2016a; Kaifu et al., 2013; Lammens and Visser, 1989; Proman and Reynolds, 2000). However, head width increases allometrically with total length (De Meyer et al., 2015, 2017a; Lammens and Visser, 1989), so larger eels may be wrongly classified as broad heads.

In contrast to the above-mentioned unimodal head-width distribution in glass eels, the head width of yellow eels has been suggested to follow a bimodal distribution (Ide et al., 2011; Kaifu et al., 2013). Bimodality would occur during the maturation stage after glass eel settlement. Six different maturation stages have been identified from the yellow eel stage onwards (Durif et al., 2005): a sexually undifferentiated yellow stage (I), a female yellow stage (FII), a female intermediate stage (FIII), two female silver eel stages (FIV and FV) and a male silver eel stage (MII). It is therefore possible that the unimodality found in glass eels shifts to bimodality during further development through these stages.

From an evolutionary point of view, variations in head shape may arise from different selective pressures at many locations, or even disruptive pressures such as observed on a side channel of the Frome River (Cucherousset

et al., 2011): individuals with intermediate traits would have a lesser fitness than individuals with more extreme traits, because they may be less efficient in the consumption of both soft/small prey and hard/large prey in comparison to the more extreme morphs (Martin and Pfennig, 2009). Head morphology may also affect an eel's fitness in yet another way: narrow-headed eels have a more hydrodynamic body shape and may therefore migrate faster or in a more energetically favourable way than broad heads (De Meyer et al., 2016; Van Wassenbergh et al., 2015), increasing their chances of successful spawning.

Despite the substantial research related to head dimorphism and studies finding evidence for bimodality, in this study, we propose the conservative null hypothesis that eels from a single river drainage do not show disruptive selection related to eel head width by assessing four sub-hypotheses: (1) Head-width variation follows a unimodal distribution, and (2) this distribution does not differ between different maturation stages; (3) body condition does not differ according to head width, and (4) eels with a narrower head width migrate at a similar speed as eels with a broader head width.

4.3 Methods

4.3.1 Study area

The River Schelde is approximately 360 km long and has a drainage area of 21,863 km^2 (Fig. 4.2). The river originates on the plateau of Saint-Quentin in France and runs through Belgium into the North Sea in The Netherlands. The Schelde is one of the few European rivers with a well-developed estuary. It is

approximately 160 km long and has a complete salinity gradient from marine to a tidal freshwater zone, including extensive freshwater, brackish and salt marshes. The Belgian part of the Schelde Estuary (i.e. the Zeeschelde) runs from Gent to Antwerp. It is well-mixed and characterized by strong currents, high turbidity and a large tidal amplitude up to 6 m (Seys et al., 1999). It has a length of 105 km, a width of 50 m to 1350 m, and an average discharge of 100 m^3 s^{-1}. In addition, several tributaries discharge into the Zeeschelde. Our study area only comprised the Zeeschelde. There is no commercial fishing in this area and fyke fishing is prohibited in Belgium since 2009, yet, recreational fishing for eels does occur.

4.3.2 Data collection

Over three consecutive years (i.e. 2015 till 2017), 272 eels were caught in summer and autumn with double fyke nets (mesh size = 8 mm) downstream the tidal weir (Merelbeke) in the freshwater part of the Zeeschelde . The dorsal view of the head was photographed with a digital camera on graph paper and several morphometric features were measured in order to determine the eel maturation stages according to Durif et al. (2005): total length (TL, to the nearest mm), body weight (W, to the nearest g), the left vertical and horizontal eye diameter (ED_v and ED_h respectively, to the nearest 0.01 mm) and the length of the left pectoral fin (FL, to the nearest 0.01 mm) (Table 4.1). Eels of all six different maturation stages were caught: sexually undifferentiated yellow eels (I, n = 51), female yellow eels (FII, n = 68), premigrant female eels (FIII, n = 91), two female silver eel stages (FIV and FV, n = 15 and n = 40, respectively) and the male silver eel stage (MII, n = 7).
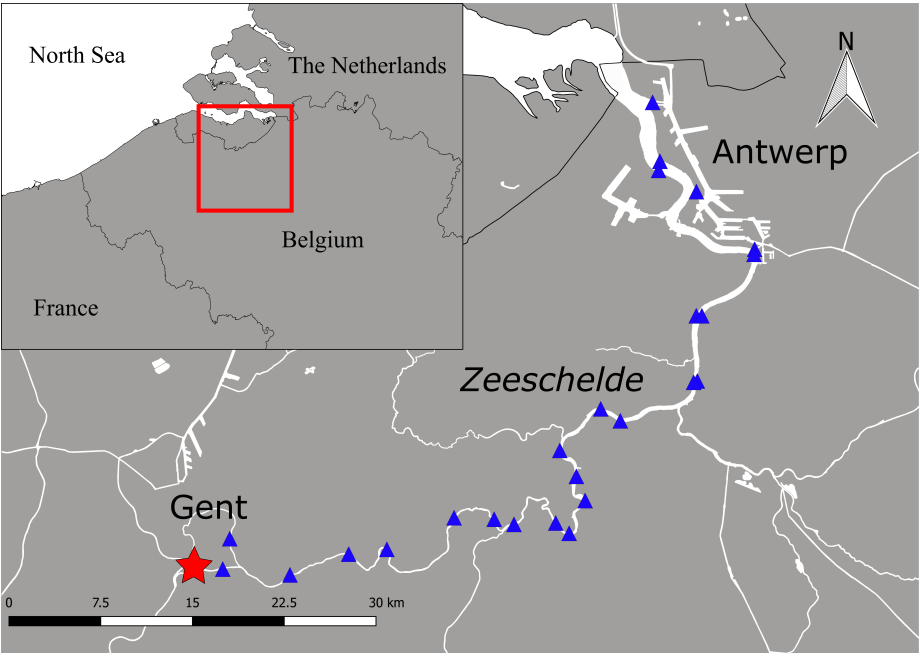
Figure 4.2: Study area with the catch location at the tidal weir in Merelbeke (asterisk) and the position of the acoustic listening stations (triangles) in the Zeeschelde.

Table 4.1: Numbers of eels caught per maturation stage with the different morphometrics: total length (TL), body weight (BW), left horizontal and vertical eye diameters (ED_h and ED_v, respectively) and left pectoral fin length (FL). Means $\pm$ SD (range) are given.

Stage	Number	TL (mm)	BW (g)	ED_h (mm)	ED_v (mm)	FL (mm)
I	51	345 ± 76	76 ± 46	4.11 ± 0.97	3.84 ± 0.92	15.42 ± 3.78
		(184 - 501)	(9 - 222)	(2.01 - 576)	(1.67-5.39)	(7.88-25.44)
FII	68	499 ± 47	213 ± 76	5.93 ± 0.48	5.51 ± 0.46	23.22 ± 2.50
		(426-642)	(88-478)	(4.66-7.02)	(4.59-6.65)	(16.68-29.98)
FIII	91	639 ± 78	504 ± 199	7.65 ± 0.70	7.14 ± 0.69	30.38 ± 3.78
		(505-835)	(141-1106)	(6.28-9.08)	(5.46-9.70)	(24.24-40.32)
FIV	15	815 ± 67	1173 ± 248	10.43 ± 0.81	9.76 ± 0.79	41.17 ± 4.54
		(707-932)	(771-1830)	(9.31-12.49)	(8.91-11.86)	(30.84-48.18)
FV	40	630 ± 70	502 ± 177	8.86 ± 0.94	8.40 ± 0.90	32.80 ± 4.03
		(510-775)	(189-912)	(7.40-11.18)	(6.95-10.39)	(25.84-45.37)
MII	7	386 ± 3	111 ± 39	6.69 ± 1.26	6.22 ± 1.09	20.06 ± 3.89
		(335-428)	(66-170)	(4.47-8.16)	(4.27-7.52)	(12.97-25.75)

4.3.3   Data analysis

Head width distribution

ImageJ (Abràmoff et al., 2004) was used to measure head width (HW) on the photographs as two times the snout length, which is defined as the distance from the midpoint between the anterior end of the eyes to the tip of the snout (Fig. 4.3). This way, HW was measured at the postorbital region where the jaw muscles can be found, an important region related to broad- and narrow-headedness (De Meyer et al., 2016). In addition, head length (HL) was measured as the distance from the tip of the snout to the start of the pectoral fins and consequently, HW/HL was calculated for each eel. Since HW/HL tends to increase slightly with TL, the unstandardized residuals were first calculated via linear regression between HW/HL and TL (see Appendix for more details). Subsequently, the residual values were used for a mixture analysis in the R environment (R Development Core Team 2017). To analyze whether the head shape variation followed a unimodal or bimodal distribution, two different penalized model selection criteria were calculated: the Akaike Information Criterion (AIC) and the Bayesian Information Criterion (BIC). Both model selection criteria are commonly applied with lower values indicating better models, but have different qualities and merits (Aho et al., 2014). Essentially, AIC is applied when the analysis is exploratory and strives for efficiency, that is, the method maximizes predictive accuracy. Consequently, AIC tends to select the most complex model as the true model (Kass and Raftery, 1995). BIC on the other hand is used for confirmatory analysis and strives for consistency (Aho et al., 2014). Related to unimodal and bimodal distribution selection, according

to Brewer (2003), a unimodal distribution is strongly and moderately suppor-
ted when ΔAIC < -8 and < -5, respectively. If ΔAIC ranges from -5 – 5, there
is equal support for both a unimodal and bimodal distribution, while values >
5 and > 8 moderately and strongly support bimodality, respectively. We used
the 'mclust' package of the R environment for model selection criterion calcula-
tion, and the 'mixtools' package for visualizations (R Development Core Team
2017).

Maturation stages and sex

First, we checked if the unimodal distribution held true for the different matur-
ation stages (I, FII, FIII, FIV, FV and MII) separately. Since the assumptions of
normality (histograms and QQ-plots) and homogeneity of variance (plotting
residuals vs. fitted values) were met (Zuur et al., 2010), a one-way ANOVA
was conducted on the residual variance of each maturation stage. Next, the
AIC and BIC were calculated for each maturation stage as mentioned above.

Body condition

To analyse if body condition changes according to HW, the relative condition
factor (Kn) (Le Cren, 1951) was used. Kn takes allometric growth into account;
when < 1, fish are in a worse condition than expected, while > 1 indicates a
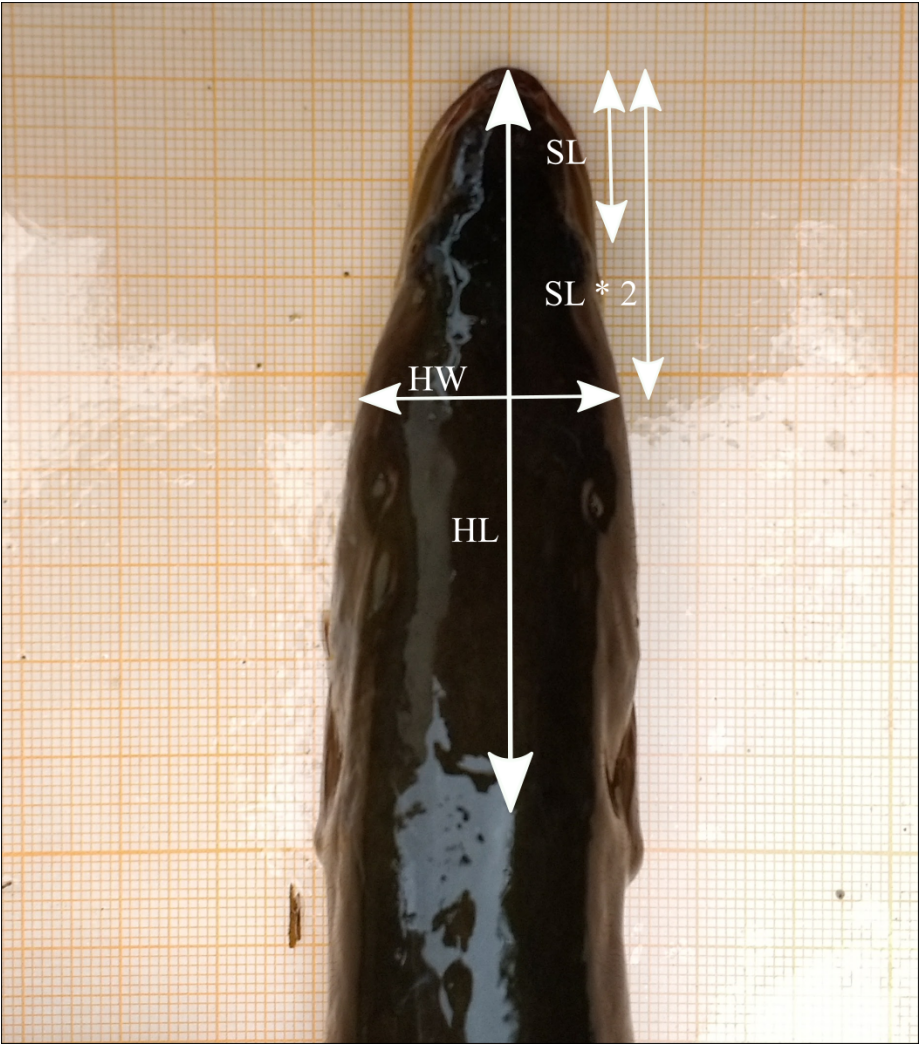better condition:

$$Kn = W/aL^b$$

Figure 4.3: Head measurements based on the dorsal picture of an eel's head on graph paper (HL: head length, HW: head width, SL: snout length).

where a is a constant and b an exponent varying from 2.5 to 4 (Hile, 1936; Martin, 1948): b = 3 indicates isometric growth and b ≠ 3 allometric growth (b < 3 for fish becoming more fusiform as they grow and b > 3 for fish becoming progressively less slender). In the formula, total length (L) and body weight (W) have a logarithmic relationship:

$$log(W) = log(a) + blog(L)$$

where b is the slope of the line and log a the intercept (Le Cren, 1951). To test if Kn changes according to HW, linear regression was applied (data followed a normal distribution and the variances were homogenous). A power analysis was conducted with the pwr R package to detect an effect of a given sample size under the 5 % significance level.

Migration speed

To determine migration speeds, 51 migrating eels were tagged with coded acoustic transmitters (V13, 13 x 36 mm, weight in air 11 g, frequency 69 kHz, estimated battery life: 1021 – 1219 days (battery lifetime depended on specific transmitter settings)) from VEMCO Ltd (Canada) and tracked in the Zeeschelde by an acoustic network of 25 ALSs (VR2W, VEMCO Ltd) (approval by the Ethical Committee of the Research Institute for Nature and Forest (ECINBO09)). After anaesthetizing the eels with 0.3 ml·L^{-1} clove oil, tags were implanted according to Thorstad et al. (2013) with permanent monofilament. Eels recovered in a quarantine reservoir for approximately one hour and were subsequently released at the ALS closest to their catch location. Data were pro-

cessed as previously described in Verhelst et al. (2018a). The residency times (i.e. the time between arrival and departure at an ALS) were calculated, which allowed us to reduce the data by accumulating the number of detections during a fixed period of time. We applied an absence threshold of one hour (i.e. the maximum time permitted between detections within a single residency period) and a detection threshold of one detection (i.e. the minimum number of detections required for a residency period). As such, the residency search resulted in intervals with arrival and departure times per eel at each ALS.

Not all eels migrated upon tagging. Therefore, an eel was considered migratory when it travelled net $\geq$ 20 km downstream during $\leq$ 40 days (Verhelst et al., 2018b). Within that period, we selected the records from the most upstream station down to the most downstream station (i.e. sometimes an eel aborted its migration and moved back upstream). The 20-km threshold is based on the maximum range distance found for yellow eels (i.e. 18 km) (Verhelst et al., 2018c) plus two times the one km detection range of an ALS in the SE (i.e. the spatial error for the migration range). The 40-days threshold is based on the finding that eels not migrating net $\geq$ 20 km downstream during that period, arrested their migration to proceed in a next season. For two eels, applying the above assumptions resulted in the selection of two migration phases per eel: they arrested their migration, subsequently moved back upstream near their catch location, and eventually resumed migration two and twelve months later. For those two eels, we only used the second migration phase for analysis. Next, we calculated the migration speed as the time needed to cross the distance between the detections at the two most distant ALSs in the migration phase. To analyse if the migration speed differed according to HW, a linear mixed effects model (transmitter ID as a random effect to account for

autocorrelation) was applied. We also applied the linear mixed effects model after removal of three extreme values. The nlme R package was used to conduct the linear mixed effects model (R Development Core Team 2017). A power analysis was conducted with the pwr R package to detect an effect of a given sample size under the 5 % significance level.

4.4 Results

4.4.1 Head-width distribution

The linear regression of the HW/HL ratio to TL proved significant (F(1, 270) = 51.26, p = 7.66e-12 with R^2 (adjusted) = 0.16), and revealed the following relationship (Fig. 4.4):

$$HW/HL\ 0.26244 + 0.00087 * TL$$

The data followed a normal distribution (Shapiro-Wilk test, W = 0.99, $p >$ 0.05), yet showed slightly right-tailed skewness. BIC proved lowest for the unimodal distribution, favoring that distribution. AIC on the other hand was lowest under the bimodal distribution, but differences between unimodality and bimodality were consistently small (Table 4.2). Moreover, when using the criteria of Brewer (2003), our data provided equal support for both unimodality and bimodality under AIC, since ΔAIC ranged between -5 and +5. However, visualization of the bimodal distribution indicated a strong overlap between the two normal distributions (i.e. one normal distribution is almost completely encompassed by the other) (Fig. 4.5). Based on these results, we

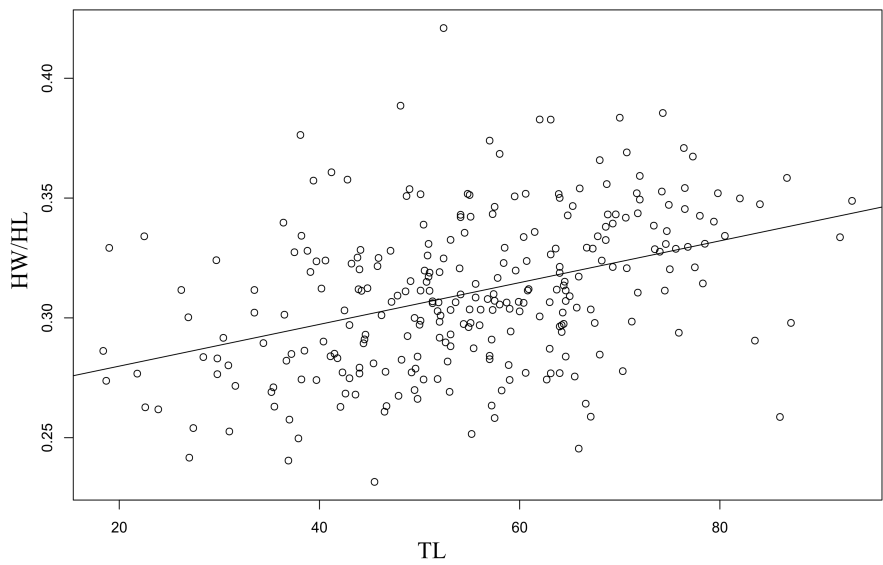concluded that a unimodal distribution best fitted our data.

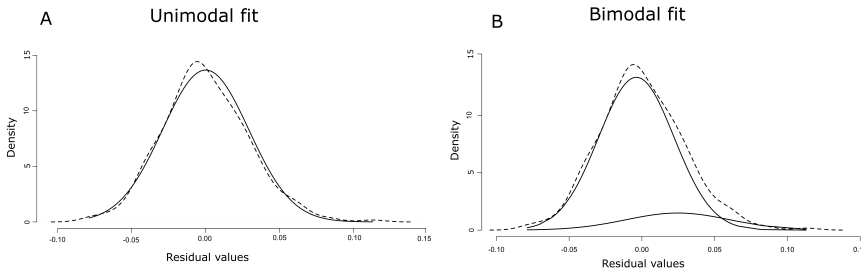Figure 4.4: Regression between the ratio head width : head length (HW/HL) and total body length (TL).

Figure 4.5: Unimodal (A) and bimodal fit (B) of normal distributions (solid lines) on the density distribution of the residuals (dashed lines).

Table 4.2: Values of the model selection criteria AIC and BIC for a unimodal and bimodal distribution.

Model selection criterion	Unimodal	Bimodal
AIC	-1148	-1149
BIC	-1141	-1134

4.4.2 Maturation stages and sex

We did not find a significant difference in residual variation between the different maturation stages (one-way ANOVA, F = 0.83, DF = 5, $p > 0.05$), although the variation for MII eels, which was based on only seven individuals, was slightly higher than for the other groups (Fig. 4.6). Similar to the total dataset and following the guidelines of Brewer (2003), BIC favored the unimodal

distribution for all stages except FII and MII, while uni- and bimodality were equally supported by AIC between eel stages (Table 4.3). Yet again, there was a strong overlap between the two normal distributions under the bimodal model (Fig. 4.7). Notably, due to the low number of observations, especially for FIV- and MII-eels, more data is needed to draw strong conclusions on the life stages.
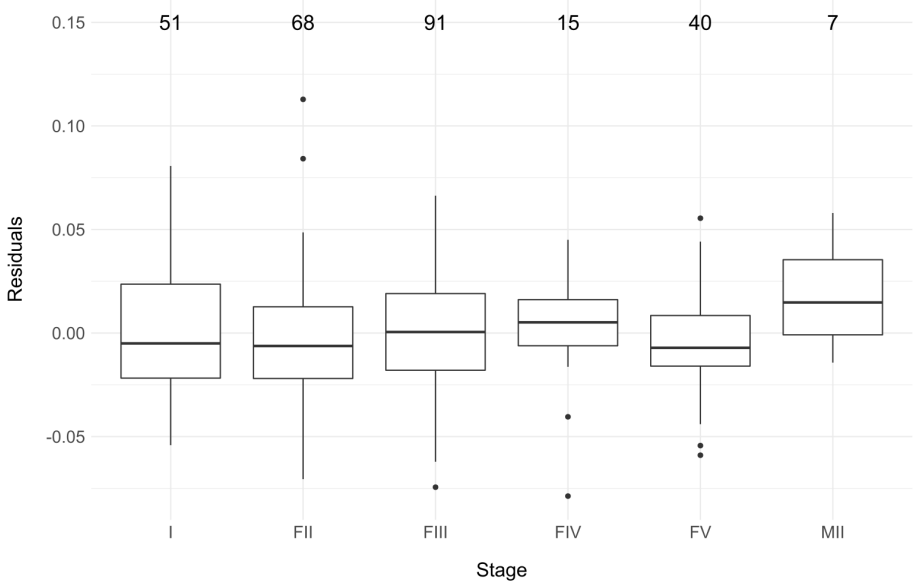

Figure 4.6: The residual variation according to the six maturation stages (I,FII, FIII, FIV, FV and MII). The number of eels per stage are indicated above the boxplot.
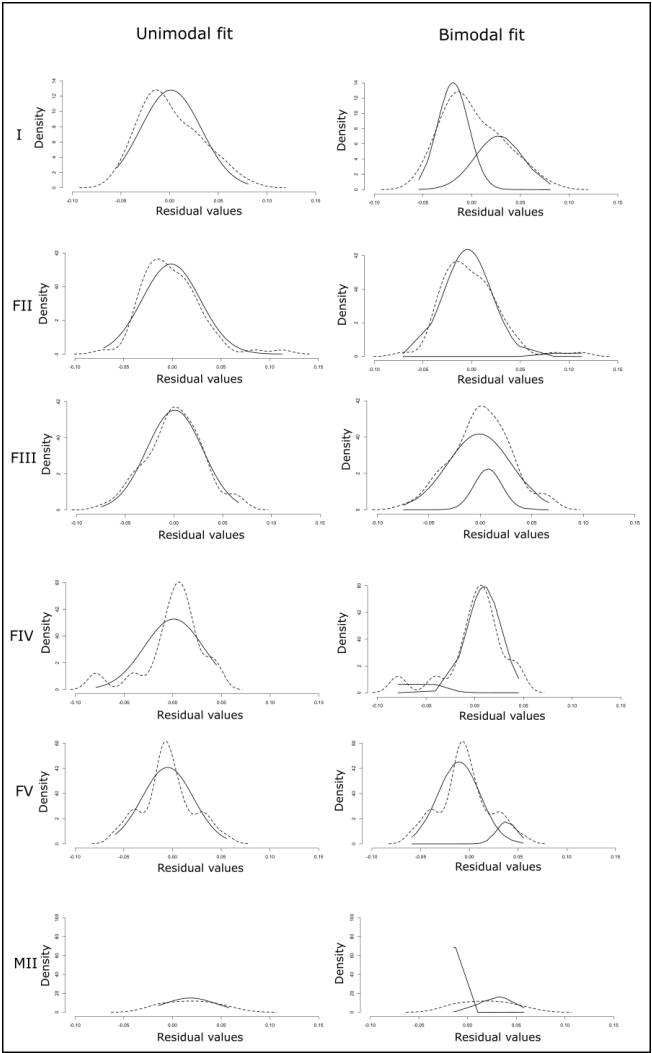
Figure 4.7: Unimodal and bimodal fit of normal distributions (solid lines) on the density distribution of the residuals (dashed lines) for each maturation stage (I, FII, FIII, FIV, FV and MII).

Table 4.3: The AIC and BIC per maturation stage (I, FII, FIII, FIV, FV and MII) for both unimodal and bimodal support.

Stage	Unimodal		Bimodal	
	AIC	BIC	AIC	BIC
I	-206	-202	-208	-200
FII	-282	-277	-288	-279
FIII	-384	-379	-380	-370
FIV	-59	-58	-60	-57
FV	-175	-171	-171	-164
MII	-28	-28	-30	-30

4.4.3   Body condition

Values for the constants a and b of the logarithmic relationship between weight and total length were a = 0.00068 and b = 3.24,

$$Kn = W/0.00068L^{3.24}$$

indicating that eels become plumpier as they grow (b > 3). Kn was on average 1.01 ± 0.15 (range: $0.51 - 1.61$) and increased significantly with a broader HW (linear regression, $F_{(1, 270)} = 6.30$, $p = 0.01$ with R^2 (adjusted) = 0.02) (power =

1.00) (Fig. 4.8):
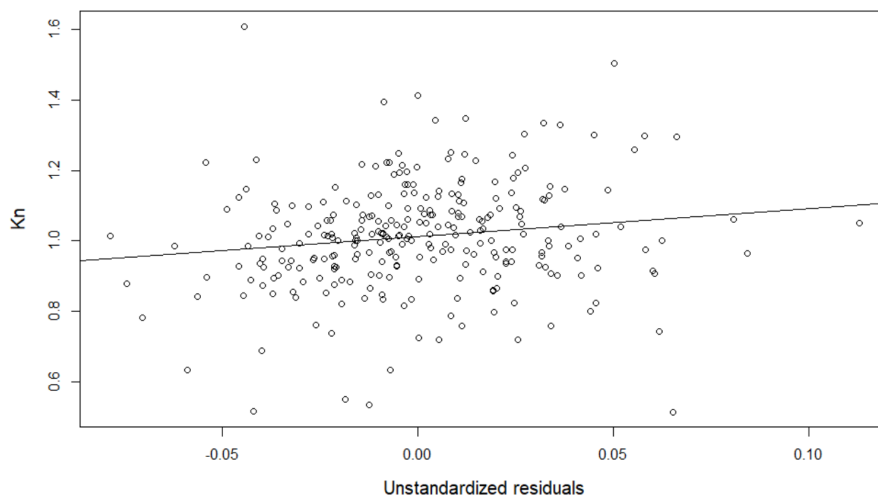
$$Kn \sim 1.01 + 0.80 * unstandardized residuals$$

Figure 4.8: The relative condition (Kn) increases with a broader head width (unstandardized residuals).

4.4.4 Migration speed

Migration speed was on average 0.05 ± 0.08 m s^{-1} (range: $0.01 - 0.40$ m s^{-1}) and did not change significantly according to HW (linear mixed effects model, t-value 0.63, DF = 49, p = 0.53; Fig. 4.9), not even after removal of the three outliers (linear mixed effects model, t-value 1.14, DF = 46, p = 0.26) (power =
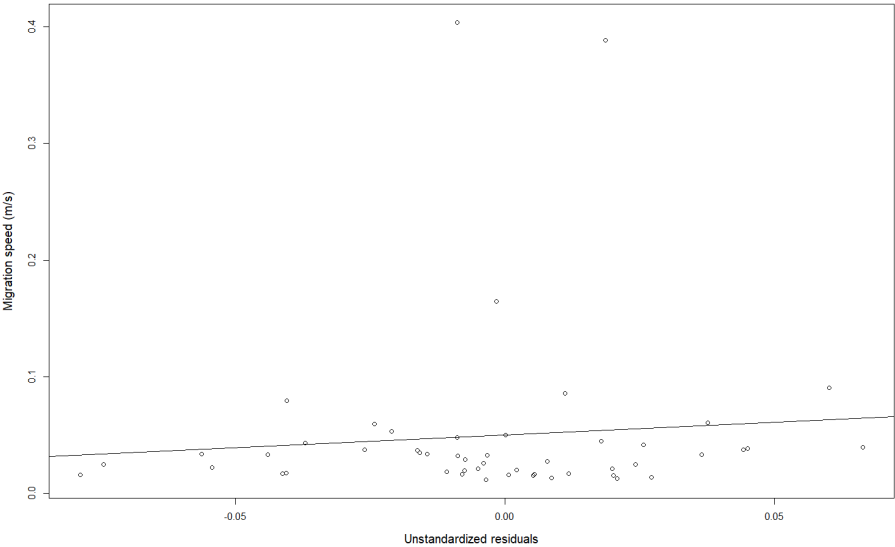
0.77).

Figure 4.9: Migration speeds in relation to the head width (unstandardized residuals).

4.5 Discussion

4.5.1 Head-width distribution

Despite the dichotomous characterization of eel HW in previous research based on eels from multiple locations and/or habitats (Ide et al., 2011; Proman and Reynolds, 2000), our study at a single location in the Zeeschelde does not support clear bimodality and hence also does not provide any in-

dication for disruptive selection. Instead, BIC indicated unimodality and AIC provided equal support for a unimodal and a bimodal distribution (Brewer, 2003). Nonetheless, AIC tends to select the more complex model over the true model (Kass and Raftery, 1995). Indeed, the equal support for both unimodality and bimodality is likely caused by the strong overlap between the two normal distributions in the bimodal model, with one normal distribution being almost completely encompassed by the other. Such overlap can hamper the distinction between a unimodal and a bimodal distribution (Hendry et al., 2006). Due to this strong overlap, we conclude that eels in the present study cannot be strictly classified into narrow- and broad-headed individuals based on a single threshold (Barry et al., 2016a; Ide et al., 2011; Lammens and Visser, 1989; Proman and Reynolds, 2000). Instead, a unimodal distribution indicates that eels have narrower or broader heads towards the extremes of a continuous normal distribution with many intermediate morphs. Notably, the slight right-skewness in the HW variation in the present study may be attributed to other selective pressures than disruptive selection. For instance, these data could be interpreted as an indication for a unidirectional pressure towards larger head widths, perhaps reflecting selection for predation on larger or hard-bodied prey. As such, skewness in one direction or the other may vary widely between locations and habitats. Although the number of eels in our study was relatively limited (n = 272), analysis of 50%, 75% and 90% of the data yielded very similar results (Fig. S1, Table S1). Moreover, the overlap between the two normal distributions under the bimodal fit tended to increase with the percentage of data taken into account (i.e. 50% to 90%), indicating a stronger support for unimodality as more data was taken into account. In addition, other studies have used similar or even lower numbers (Barry et al., 2016a; Cucherousset

et al., 2011; Kaifu et al., 2013; Proman and Reynolds, 2000).

(Ide et al., 2011) did find evidence of bimodality and observed that head shape variation in European eel in Belgium was best described by two unimodal distributions with overlapping tails. This discrepancy may be explained by the fact that these authors covered different sampling locations, often characterized by different feeding conditions. If head shape depends on prey type, then eels caught at locations with a higher abundance of soft-bodied/small prey will tend to the narrow side of the HW distribution, while the opposite will hold true for locations dominated by hard-bodied/large prey. When eels of two such contrasting locations are pooled together, a bimodal distribution would be more likely to occur.

Under the assumption that HW distribution is mainly the result of food choice (Lammens and Visser, 1989; Proman and Reynolds, 2000), the observed unimodal distribution in the Zeeschelde could be explained by an opportunistic behaviour of eels (Lammens et al., 1985; Schulze et al., 2004; Van Lieferinge et al., 2012). Feeding on a wide range of prey items reduces selective pressures towards head shapes that are more specialized for the consumption of either hard or soft prey. Predatory fish of cold-temperate waters tend to be opportunistic feeders, as productivity in these areas is often relatively low and prey abundance depends on season and temperature (Keast, 1979), implying that the most available prey has the highest chance of being consumed. However, eels can also display a remarkable preference for specific prey items, irrespective of their availability (Barak and Mason, 1992).

Other factors than food could also explain the occurrence of head dimorphism: narrow headed eels have been suggested to be more crepuscular and for-

age in the littoral zone, while broad headed eels would be more active at night and in the limnetic zone (Barry et al., 2016a; Cucherousset et al., 2011). In addition, bimodality may be present mostly in areas where eel densities are high, leading to intraspecific competition through resource polymorphism and consequently to different head shapes (e.g. in lakes with artificially stocked eels) (Lammens and Visser, 1989).

4.5.2 Maturation stages, sex and body condition

Eel maturation stages are commonly classified according to Durif et al. (2005) (Barry et al., 2016a; Bultel et al., 2014; Stein et al., 2015). Although the method may not be 100% conclusive, distinction between male and female silver eels was confirmed in our study as males showed the typical silvering characteristics (visible lateral line, large, melanised pectoral fins, dark dorsal side, silver-white ventral side and large eyes) and had a TL < 45 cm (Tesch, 2003).

De Meyer et al. (2015) hypothesized that the absence of a clear bimodal pattern in glass eels, contrasting with its presence in yellow eels (Ide et al., 2011), may be attributed to a trophic niche segregation between different eel developmental stages. However, we found no bimodal pattern in the Zeeschelde in any of the maturation stages defined by Durif et al. (2005). Like for the total dataset, BIC favored a unimodal distribution and AIC provided equal support for a unimodal and a bimodal distribution. Again, the latter likely results from the strong overlap between two normal distributions. Given the small number of specimens in the present study, especially in FIV (15) and MII (7) eels, we can, however, not rule out the possibility that the distribution could be skewed due to the tail of the distribution (Hendry et al., 2006). The absence of a clear

bimodal distribution could again be explained by the opportunistic behavior of the eels (Lammens and Visser, 1989; Schulze et al., 2004; Van Liefferinge et al., 2012). Specifically, since our study included eels from a single location only, opportunistic feeding and low to moderate population density would render disruptive selection pressure towards feeding specificity unlikely during the different maturation stages in the Zeeschelde.

Counter to Cucherousset et al. (2011), who argued that the better body condition of both narrow and broad headed eels compared to intermediate headed eels was the result of disruptive selection (Martin and Pfennig, 2009; Skulason and Smith, 1995), body condition of eels in the Zeeschelde also did not support the idea of disruptive selection, since body condition increased along with HW, suggesting unidirectional selection. However, the small amount of variation explained by the model suggests that factors other than head width play a more prominent role in body condition variation.

4.5.3   Migration speed

Combining telemetry with HW classification, Barry et al. (2016a) observed a larger home range for broad headed yellow eels. In addition, circadian activity patterns differed, with narrow-headed yellow eels being more crepuscular while broad-headed yellow eels more nocturnal. Here, we preliminarily analysed if the downstream migration speed (i.e. movement at meso-scale) of silver eels in the Zeeschelde differed according to HW. Migration speed is often calculated to make predictions about progression (Aarestrup et al., 2010; Breukelaar et al., 2009; Bultel et al., 2014), swimming performance (Russon et al., 2010; Van Den Thillart et al., 2004; van Ginneken et al., 2005) or the chances

of reaching the spawning area in time (Righton et al., 2016). Our results suggest that at least the progression of silver eels is not influenced by their head morphology. Nonetheless, swimming experiments in swim tunnels may shed more light on the relationship between HW and different aspects of migration and swimming performance (van Ginneken et al., 2005).

4.6 Conclusion

In contrast to evidence for a bimodal head-width distribution of European eel (Ide et al., 2011), we found support for a unimodal distribution in European eel HW variation at a location in the Zeeschelde, both when separately analyzing different maturation stages and when looking at the total dataset. This indicates a lack of evidence for disruptive selection but does not exclude unidirectional pressures on variation in eel head shapes. Finally, downstream migration speed of silver eel at a meso-scale was not influenced by HW morphology. We conclude that eels in the Zeeschelde could not be dichotomously classified into narrow and broad heads, but rather represent a continuum of specimens with narrow to broad heads following a normal distribution.